Critical Behavior of Symmetrical Fluid Mixtures in Random Pores

Pier Giorgio De Sanctis Lucentini[1,*] and Giuseppe Pellicane[2,†]

[1]Dipartimento di Fisica, Università degli Studi di Roma, Piazzale Aldo Moro 2, 00185 Roma, Italy
[2]Dipartimento di Fisica, Università degli Studi di Messina, Contrada Papardo, 98166 Messina, Italy

(Received 24 June 2008; published 10 December 2008)

We study the liquid-liquid demixing of a binary mixture with a symmetrical coupling to the quenched disorder by means of computer simulation. The critical point in the thermodynamic limit is estimated both by assuming the knowledge of the critical exponents and independently of them. The finite-size scaling analysis of the susceptibilities and the values of the critical amplitudes show that the universality class of the fluid mixture is compatible with the diluted quenched-Ising model. Our findings extend the class of systems exhibiting the same critical behavior of diluted antiferromagnets.

DOI: 10.1103/PhysRevLett.101.246101 PACS numbers: 68.35.Rh, 64.75.−g, 64.75.Gh

During the past decades, a number of experiments on binary fluid mixtures adsorbed in porous disordered materials, including glasses [1–3], gels [4], and metals [5], has shown that the phase behavior can be quite different from the bulk case. Though deviations of the critical parameters in the presence of fluid-pore wall interactions are somewhat expected, the assessment of the nature of the phase transitions has been an elusive goal for a long time [4,6]. The ubiquitous long-time relaxation and the resulting difficulty to observe a macroscopic phase separation on a measurable time scale are explained mainly in the framework of the random field Ising model (RFIM) [7]. Very recently, Vink, Binder, and Löwen [8] used computer simulation to suggest that colloid-polymer mixtures trapped in colloidal matrices could be promising candidates to observe a genuine RFIM behavior. The fluctuations of the local chemical potential $\mu(\vec{r})$ of the fluid, originated by the size polydispersity of the random pores, are the counterpart of the random magnetic fields h_i of the RFIM. For binary mixtures, this mechanism is driven by the preferential interaction of one of the two species with the pore walls. Fluctuations of $\mu(\vec{r})$ are expected to act as a random field only when $\xi \gg \bar{R}$, where ξ is the correlation length of the relevant order parameter and $\bar{R}$ is the average radius of the pore cavity. To date, this condition has never been achieved experimentally because ξ tends to round off near the critical point at a value that is of the order of the pore size, e.g., $\xi \approx 30$–35 Å in silica aerogels [9] or $\xi <$ 70 Å in Vycor glass [3]. The difficulty to sense the disorder of the confining material on distances longer than the pore width is not completely understood [3]. A plausible explanation of this drawback is found in the wetting transition on the surface of the walls of one of the two components [2,3] or of the denser phase of the liquid-gas transition [6,9]. Wetting suppresses critical fluctuations and promotes a microphase separation inside the single cavities of the random matrix [10]. Both RFIM and wetting hinge upon the same physical argument, i.e., preferential adsorption of one of the two components on the solid host [7,10]. Accordingly, two features can be predicted at the same time when favorable fluid-matrix interactions are absent: The role of wetting in preventing the macroscopic phase separation should be milder, and the RFIM conjecture is not valid anymore. Thus, a fundamental issue is to determine the universality class of a binary fluid mixture in which the two species interact similarly with the pore walls.

In this Letter, we report evidence for a binary mixture in the presence of random pore walls that the critical behavior is in agreement with the one predicted for the weakly diluted quenched-Ising model, or random Ising model (RIM) [11,12], provided the interaction parameters are invariant with respect to the interchange of the particle species. The RIM is the universality class of a ferromagnetic material weakly diluted with a nonmagnetic component far from the percolation threshold. In order to figure out this result, it is useful to consider a lattice-gas model in the presence of correlated random fields, such as the one reported in Ref. [13], and the usual equivalence with a spin-1/2 model. In the absence of random fields, one recovers the diluted quenched-Ising model, but without hole-particle symmetry due to fluid-matrix interactions. Here we consider a continuum model of a binary fluid mixture, namely, a symmetrical, nonadditive hard-sphere mixture (NAHSM), where the diameters of species 1 and 2 are, respectively, $\sigma_1 = \sigma_2 = \sigma$ and the cross interaction σ_{12} is determined by the positive value of the nonadditivity parameter Δ: $\sigma_{12} = 0.5(\sigma_1 + \sigma_2)(1 + \Delta)$. Bulk symmetrical NAHSMs always exhibit a demixing transition, and their critical point has been recently demonstrated to be of the Ising type [14]. We adopt, as a model for the diluted disorder, an ensemble of ''frozen'' spatial configurations of hard-sphere particles of diameter $\sigma_0 = \sigma$. Our system features a fluid mixture with symmetrical fluid-pore wall interactions and in the presence of quenched disorder [8,13]. Besides the statistical average over the configurations of the fluid molecules, thermodynamic quantities are calculated by averaging over a number of spatial realiza-

tions of the matrix. In our calculations, we fix $\Delta = 0.2$, the reduced number density of the matrix $\rho_0\sigma^3 = (N_0/V)\sigma^3 = 0.1$, and we use σ as unit of length. As outlined before, no random fields can be associated with our model, and the phase coexistence always satisfies the two symmetrical relations $x_1^{\mathrm{I}} = x_2^{\mathrm{II}}$ and $x_2^{\mathrm{I}} = x_1^{\mathrm{II}}$, where x_β^α is the composition of the species labeled β in the α phase. For symmetrical mixtures, these relations imply that the critical composition is $x_c = (N_1/N)_c = 0.5$. We performed a finite-size scaling analysis of the liquid-liquid phase separation for a number of particles $N = 256$, 500, 1000, 2048, 4000, and 10000, by means of semigrand canonical ensemble Monte Carlo [14] computer simulations [15]. The most useful quantity to study the phase separation is the probability distribution $[P_N(m)]_{qa}$ of the order parameter $m = |x - 0.5|$ averaged over different matrix realizations ($[\cdots]_{qa}$), where the composition is x and m plays the same role of the magnetization in antiferromagnetic materials. Far below the critical density ρ_c^N, $[P_N(m)]_{qa}$ exhibits a single peak centered around the equimolar composition $x = 0.5$. Close to and above ρ_c^N, $[P_N(m)]_{qa}$ separates into two distinct peaks, which are symmetrical with respect to the equimolar composition. By increasing the number of realizations of the matrix n_0, we experienced a rapid convergence of the normalized histogram $[P_N(m)]_{qa}$ to a smooth shape. We estimated $[P_N(m)]_{qa}$ by averaging over $n_0 \geq 60$. We note that the shape of $[P_N(m)]_{qa}$ does not exhibit any trace of violation of hyperscaling at the critical point, as was shown in Ref. [8] for a system experiencing an asymmetric coupling with the matrix. We also estimated the critical $[P_N(m)]_{qa}$ at $\rho_0\sigma^3 = 0.3$ and found a similar shape. For each system size, when the critical point is nearly approached from the two-phase region, m should vanish according to the power law $m \propto t^\beta$, where β is the critical exponent associated with the order parameter and $t = |\frac{\rho}{\rho_c(N)} - 1|$. The shape of the curves reported in Fig. 1 shows finite-size deviations, especially close to the critical point. A different power law which takes into account such deviations is $\rho_c(N) - \rho_c(\infty) \propto N^{-(1/3\nu)}$, where ν is the critical exponent related to the divergence of the correlation length and $\rho_c(\infty)$ is the critical density in the thermodynamic limit ($N \to \infty$). In order to ascertain the universality class of the system, we assumed *a priori* that the symmetrical NAHSM belongs to the RIM universality class and used the predictions of finite-size scaling theory to verify this hypothesis. The estimate of $\rho_c(N)$ and $\rho_c(\infty)$ was based on the analysis of the simulation points close to the critical point by means of the power laws. In this Letter, we always adopted values of the most recent RIM critical exponents reported in the review by Hasenbusch *et al.* [12], i.e., $\beta = 0.354(1)$ and $\nu = 0.683(2)$. The curves in Fig. 1 testify to the quality of the fit of the simulation data close to the critical point. In the inset in Fig. 1, we report the size-dependent $\rho_c(N)$ as a function of $N^{-(1/3\nu)}$. As expected, the data are consistent

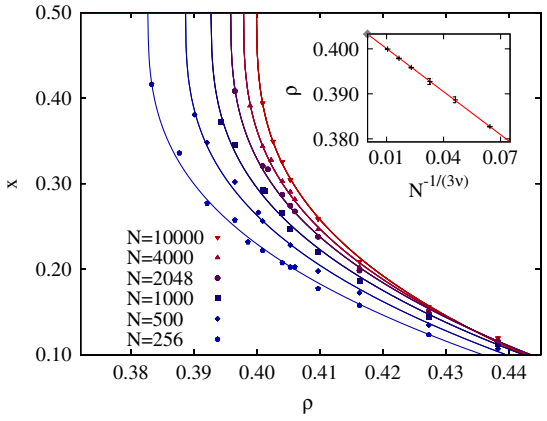

FIG. 1 (color online). Composition versus reduced density phase coexistence curves for different system sizes. Power-law curves are fits of the simulation data close to the critical point. Inset: Critical densities as a function of $N^{-(1/3\nu)}$.

with the power law of the correlation length, and the extrapolation of the linear fit (full line) to zero gives as an estimate of the critical density in the thermodynamic limit $\rho_c^{(1)} = 0.4033(3)$.

To locate the critical point, we also studied the N dependence of the Binder cumulant [16] $U_4 = 1 - \frac{[\langle m^4\rangle]_{qa}}{3[\langle m^2\rangle]_{qa}^2}$, where $\langle\cdots\rangle$ is the statistical average over the microstates of a single matrix realization. This quantity should become size-independent at the critical point; hence, in the scaling regime (for sufficiently high N), plots of U_4 as a function of the density are expected to have a common intersection point, which is indicative of the critical density [16]. According to Hasenbusch *et al.* [12], the universal value of U_4 at the critical density for the RIM is $U_4^* = 0.451(1)$ (see the horizontal line in Fig. 2). As shown in Fig. 2, the intersections of the Binder cumulants occur at a slightly different value of U_4. Corrections to finite-size scaling of

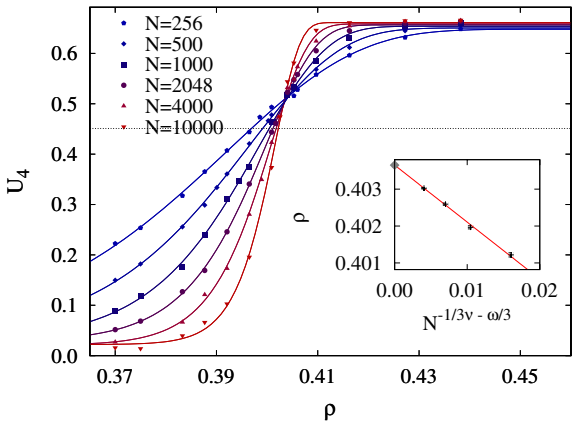

FIG. 2 (color online). Binder cumulant U_4 values for different system sizes (curves are guidelines for the eye). The horizontal line is the universal value of U_4 for the RIM [11]. Inset: Size-dependent critical densities (see text) as a function of $N^{-(1/3\nu)-(\omega/3)}$.

U_4 in the neighborhood of the critical density should explain the observed shift, which comes out size-independent for the considered N range [14,16]. Thus, the critical density can be unambiguously determined at the crossing point of the Binder cumulants (see Fig. 2) as $\rho_c^{(2)} = 0.4034(1)$ [12]. We note that the latter estimate of $\rho_c(\infty)$ is completely free from any assumptions concerning the universality class of the system.

Then we evaluate the critical densities [14] $\rho_c^*(N)$ as intersection of the Binder cumulants with the horizontal line $U_4 = U_4^*$ (see Fig. 2). For the size-dependent critical densities, the scaling behavior is $\rho_c^*(N) - \rho_c(\infty) \propto N^{-(1/3\nu)-(\omega/3)}$ [16], where $\omega = 0.33(3)$ is the correction to the scaling exponent [12]. The critical densities for the four higher sizes are reported in the inset in Fig. 2 and are in agreement with the expected scaling behavior. The extrapolation of the linear fit to the thermodynamic limit gives $\rho_c^{(3)} = 0.4037(1)$, which is consistent with the previous estimates. In order to verify whether the assumed universality class is correct for our system, we exploited the scaling behavior of the susceptibility [8] $\chi_N/V = [m^2]_{qa} - [m]_{qa}^2$ around the critical point. χ_N is a second-order moment of $[P_N(m)]_{qa}$, and it is supposed to be more sensitive than m to variations of the critical exponents. Finite-size scaling theory [16] predicts that, in the neighborhood of the critical point, $\chi_N = N^{(\gamma/3\nu)}\chi_0(tN^{(1/3\nu)})$, where χ_0 is a scaling function which is assumed to be system size-independent and $\gamma = 1.341(4)$ is the RIM exponent associated to the susceptibility [12]. Thus, plots of $N^{-(\gamma/3\nu)}\chi_N$ vs $tN^{(1/3\nu)}$ should collapse onto a master curve, provided the RIM critical exponents [11] and the estimate of the critical density in the thermodynamic limit are used. We used the estimates $\rho_c^{(1)}$, $\rho_c^{(2)}$, and $\rho_c^{(3)}$ in the scale factor, and we calculated the susceptibility approaching the critical point both from the one-phase region and from the two-phase region. The scaling plots of the susceptibility at $\rho_c^{(1)} = 0.4033$ are presented in Fig. 3 for the four higher system sizes considered in this work. The coalescence of the data on a master curve is an evident signature of RIM critical behavior. According to the basic theory of critical phenomena, the susceptibility should diverge as $\chi = \Gamma t^{-\gamma}$ at the critical point, with a value of the critical amplitude Γ different when approaching the critical density for $\rho > \rho_c(\infty)$ or for $\rho < \rho_c(\infty)$. The ratio between the critical amplitudes in the one-phase region (Γ^+) and in the two-phase region (Γ^-) is a universal quantity, e.g., for the 3D Ising universality class is $\frac{\Gamma^+}{\Gamma^-} = 4.76(24)$ [12]. As shown in Fig. 3, for large $tN^{(1/3\nu)}$ the data match the power-law behavior expected in the thermodynamic limit. Thus, it is convenient to use the critical amplitude as a single free parameter to fit a line with slope $-\gamma$ on the scale of Fig. 3. The fitted values of the critical amplitudes are presented in Table I. The ratios of the critical amplitudes for different estimates of $\rho_c(\infty)$ are reported in Table II. Remarkably, as shown in Table II, these estimates are consistent both with experimental measurements on antiferromagnets resembling the RIM [17–19] and with field-theoretical determinations [20]. A subtle issue to be addressed is the possibility to discriminate, within our finite-size scaling analysis, between the relatively small differences of the critical exponents of the RIM and of the 3D Ising model. To this aim, we repeated again the previous analysis in order to estimate the critical points $\rho_c^{(1)}$ and $\rho_c^{(3)}$ with the 3D Ising model critical exponents $\beta = 0.3258(1)$, $\nu = 0.6304(13)$, and $\omega = 0.845(10)$ and with $U_4^* = 0.465(1)$ [12]. The new estimates of the critical points are reported in Table I. Then we considered the effect of scaling the susceptibilities for both these critical points and for $\rho_c^{(2)}$, with ν and $\gamma = 1.2396(1)$ of the 3D Ising model. We observed a neat worsening of the scaling of the susceptibilities in each of the three cases. We estimated quantitatively the consistency of the 3D Ising model with our data by calculating the critical amplitudes, which are reported in Table I. The ratios of the critical amplitudes in Table II are very different from the expected universal value for the 3D Ising class. Thus, the present analysis rules out the consistency of our system with the critical exponents of the 3D Ising model.

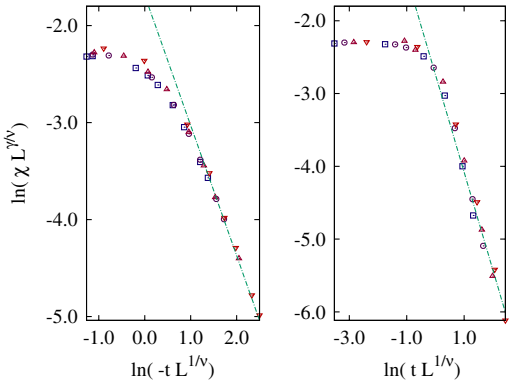

FIG. 3 (color online). Log-log $N^{-(\gamma/3\nu)}\chi_N$ vs $tN^{(1/3\nu)}$ scaling plot of the susceptibility for $\rho_c^{(1)} = 0.4033$. The legend is the same as the previous figures. Results are reported in the one-phase (left panel) and two-phase regions (right panel). The lines are the power laws $\chi = \Gamma^+ x^{-\gamma}$ (left panel) and $\chi = \Gamma^- x^{-\gamma}$ (right panel), where Γ^+ and Γ^- have been used as fit parameters to the simulation data for large $tN^{(1/3\nu)}$.

TABLE I. Critical densities as calculated by different methods and related critical amplitudes.

	$\rho_c(\infty)$	Γ^+	Γ^-
	0.4033(3)	0.188(3)	0.072(4)
RIM	0.4034(1)	0.189(3)	0.071(3)
	0.4037(1)	0.185(3)	0.065(2)
	0.4032(1)	0.234(4)	0.094(6)
3D Ising	0.4034(1)	0.236(4)	0.093(6)
	0.4027(1)	0.226(4)	0.101(7)

TABLE II. Amplitude ratios $\frac{\Gamma^+}{\Gamma^-}$ for different systems. NAHSMs are the estimates of this work obtained by using the critical densities $\rho_c^{(1)}$, $\rho_c^{(2)}$, and $\rho_c^{(3)}$ reported in Table I. RG denotes renormalization group.

	NAHSM ($\rho_c^{(1)}$)	NAHSM ($\rho_c^{(2)}$)	NAHSM ($\rho_c^{(3)}$)	$Fe_{0.46}Zn_{0.54}F_2$	$Mn_{0.75}Zn_{0.25}F_2$	$Fe_{0.5}Zn_{0.5}F_2$	RG
RIM	2.61(17)	2.66(17)	2.86(16)	2.8(2)[a]	2.56(15)[b]	2.2(1)[c]	3.05(32)[d]
3D Ising	2.49(20)	2.53(20)	2.23(20)				4.76(24)[e]

[a]Experimental measures from Ref. [17].
[b]Experimental measures from Ref. [18].
[c]Experimental measures from Ref. [19].
[d]RG theory estimate for the RIM and for the 3D Ising model from Ref. [20].
[e]RG theory estimate for the RIM and for the 3D Ising model from Ref. [12].

In summary, the results of the scaling analysis provide new evidence of RIM behavior also for symmetrical fluids in the presence of quenched disorder. Pore walls lacking a preferable mechanism of interaction with one of the species of the fluid mixture could be engineered in the realm of colloid science. Colloidal particles with controlled size and shape can be intercalated as functional guest molecules in hydrogel scaffolds or in silica sol, and highly open-cell pores have been recently obtained [21]. The nature of the surface interactions of the immobilized colloidal particles can be tuned by infiltrating the matrix with sol-gel solutions or by chemical treatment [22]. A prototype of a symmetrical fluid mixture could be realized with colloidal particles by coating their surfaces with immiscible polymer brushes of different type and chain length [23]. The mesoscopic character and the tunability of the interactions of these systems make them good candidates to study the critical behavior with a range of experimental techniques. The possibility to gradually change the fluid-wall interactions in colloidal systems could allow experimental access to the crossover regime from the RIM to the RFIM also in fluids adsorbed in random pores, similarly to what is achieved in dilute anisotropic antiferromagnets by gradually turning on a uniform magnetic field [24]. As far as the absence of selective adsorption is concerned, we believe that a proper tailoring of the interactions could reduce the wetting of one of the two components on the pore walls, which depletes the fluid and reduces the volume available for phase separation [2,3,9]. Thus, the resulting enhancement of the critical fluctuations could allow correlation lengths spanning several pores and promote a macroscopic phase separation, which eventually could make it easier to observe the RIM behavior.

We are grateful to K. Binder, C. Caccamo, P. V. Giaquinta, A. Pelissetto, A. Scala, F. Sciortino, P. Tartaglia, and R. L. C. Vink for useful discussions and for valuable comments on the manuscript.

*pier.giorgio.desanctislucentini@roma1.infn.it
†Corresponding author.
gpellicane@unime.it

[1] M. C. Goh, W. I. Goldburg, and C. M. Knobler, Phys. Rev. Lett. **58**, 1008 (1987); S. B. Dierker and P. Wiltzius, Phys. Rev. Lett. **58**, 1865 (1987); P. Wiltzius, S. B. Dierker, and B. S. Dennis, Phys. Rev. Lett. **62**, 804 (1989); S. Lacelle *et al.*, Phys. Rev. Lett. **74**, 5228 (1995).
[2] B. J. Frisken, F. Ferri, and D. S. Cannell, Phys. Rev. Lett. **66**, 2754 (1991).
[3] M. Y. Lin *et al.*, Phys. Rev. Lett. **72**, 2207 (1994).
[4] J. V. Maher *et al.*, Phys. Rev. Lett. **53**, 60 (1984).
[5] D. J. Tulimieri, J. Yoon, and M. H. W. Chan, Phys. Rev. Lett. **82**, 121 (1999).
[6] A. P. Y. Wong *et al.*, Phys. Rev. Lett. **70**, 954 (1993).
[7] P. G. de Gennes, J. Phys. Chem. **88**, 6469 (1984).
[8] R. L. C. Vink, K. Binder, and H. Löwen, Phys. Rev. Lett. **97**, 230603 (2006); arXiv:0804.1967v1.
[9] Y. B. Melnichencko *et al.*, Phys. Rev. E **69**, 057102 (2004).
[10] A. J. Liu *et al.*, Phys. Rev. Lett. **65**, 1897 (1990).
[11] H. G. Ballesteros *et al.*, Phys. Rev. B **58**, 2740 (1998).
[12] M. Hasenbusch *et al.*, J. Stat. Mech. (2007) P02016; A. Pelissetto and E. Vicari, Phys. Rep. **368**, 549 (2002).
[13] E. Kierlik *et al.*, Mol. Phys. **95**, 341 (1998).
[14] W. Góźdź, J. Chem. Phys. **119**, 3309 (2003).
[15] Fluid particles are inserted into the cavities of the matrix and equilibrated for 10^5 Monte Carlo cycles (MCCs). Quantities of interest are collected over 10^6 MCCs. For selected states close to the critical point, the number of cumulation cycles was extended well beyond 10^6 MCCs. Each cycle consists of N attempts to displace or to exchange the identity of the particles of the binary mixture, and the ratio between the two moves varies according to the proximity to the critical point.
[16] K. Binder, Z. Phys. B **43**, 119 (1981).
[17] D. P. Belanger, A. R. King, and V. Jaccarino, Phys. Rev. B **34**, 452 (1986).
[18] P. W. Mitchell *et al.*, Phys. Rev. B **34**, 4719 (1986).
[19] R. J. Birgenau *et al.*, Phys. Rev. B **27**, 6747 (1983).
[20] C. Bervillier and M. Shpot, Phys. Rev. B **46**, 955 (1992).
[21] E. C. Cho *et al.*, Nano Lett. **8**, 168 (2008); C. A. Morris, Science **284**, 622 (1999); D. F. Schmidt *et al.*, Chem. Mater. **20**, 2851 (2008).
[22] R. A. Caruso and M. Antonietti, Chem. Mater. **13**, 3272 (2001); D. J. Durian and C. Franck, Phys. Rev. Lett. **59**, 555 (1987).
[23] Y. Hennequin, M. Pollard, and J. S. van Duijneveldt, J. Chem. Phys. **120**, 1097 (2004).
[24] P. Calabrese, A. Pelissetto, and E. Vicari, Phys. Rev. B **68**, 092409 (2003).